Transient-state feasibility set approximation of power networks against disturbances of unknown amplitude

Yifu Zhang and Jorge Cortés

***Abstract*— This paper develops methods to efficiently compute the set of disturbances on a power network that do not tip the frequency of each bus and the power flow in each transmission line beyond their respective bounds. For a linearized power network model, we propose a sampling method to provide superset and subset approximations with a desired accuracy of the set of feasible disturbances. We also introduce an error metric to measure the approximation gap and design an algorithm that is able to reduce its value without impacting the complexity of the resulting set approximations. Simulations on the IEEE 118-bus power network illustrate our results.**

I. Introduction

The stability of electrical power networks and their robustness against voltage and frequency fluctuations is key in the operation and management of the current power grid. Transient stability, as the major stability problem in power network analysis, has attracted much focus from both industry and academia. In general, transient stability refers to the ability of power networks to reach an acceptable state range when subjected to disturbances while respecting operational constraints. Due to the uncertainty and variety of disturbances, it is challenging to characterize the disturbances under which power networks can still operate normally during transients. This is what motivates our work.

Literature review: The study of stability margins and robustness against disturbances is critical in power networks. There are two major methods [1], [2] for analyzing transient stability: the time-domain method and the direct method. The time-domain method usually refers to the numerical simulation of the system behavior for some specific disturbance. Depending on the numerical solver, this method is able to consider almost any power network models and to precisely depict the state trajectories, provided that the system parameters are accurately known. However, the time-domain method cannot answer question regarding how far the system is from (in)stability and can hardly provide guidelines for control [3]. The direct method [4], [5], based on Lyapunov stability analysis, focuses on estimating the region of attraction of the system equilibrium using Lyapunov functions to ensure the stability of the power networks without knowing the specific form of the disturbances (provided the initial state lies in the identified region). Most of the direct methods require less simulation time than time-domain methods and, more importantly, are able to provide a stability margin and parameter sensitivity analysis. However, due to the difficulty of finding Lyapunov functions and the conservativeness required in bounding their evolution, especially for large-scale power networks with complex dynamics, the identified regions of attraction could be poor approximations of the real one. We see the characterization of the transient-state feasibility set tackled here as a building block towards the development of metrics and methods that can serve to quantify the robustness of power networks. If a description of a region under which the overall system performs satisfactorily can be obtained, a robustness metric can then be defined as the minimum disturbance that is able to force the system move out of that region, see e.g., [6], [7]. Such metrics are key in determining why and how failure can happen, and preventing cascading failures.

Statement of contributions: We consider a linearized AC power network model with unknown amplitude and time-varying power disturbance injected at various buses. For a given period of time, if the frequency of each bus and the power flow in each transmission line still remain in their respective bounds, then we term this disturbance feasible for the transient stability of the power network. Our main goal is to design efficient ways of computing the transient-state feasibility set consisting of all such disturbances. Since this set contains infinitely many constraints, our first contribution develops a sampling method to approximate it by identifying a subset and a superset. We compute the subset approximation by sampling and tightening the constraints at finite discrete-time instants, and using the linear dynamics of the network to upper and lower bound the evolution of state signals, so as to ensure that all constraints are respected at all times. The superset approximation comes from using only a finite number of the constraints appearing in the exact set. We show that the approximation sets converge to the real transient-state feasibility set as we increase the number of sampling points. Our second contribution consists of defining a metric to measure the approximation conservativeness by estimating the region difference between the approximations and the real set. Finally, our last contribution is to design an algorithm to optimize this metric by adjusting the positions of the sampling points in a way that monotonically decreases the value of the error metric. Various simulations illustrate our results. For space reasons, all proofs are omitted and will appear elsewhere.

II. Preliminaries

This section introduces basic notation and notions from algebraic graph theory and set limit.

1) Notation: Let $\mathbb{R}$ and $\mathbb{N}$ denote the set of real and natural numbers, respectively. Variables are assumed to belong to the Euclidean space if not specified otherwise. Denote by $a \leqslant b$ $(<, \geqslant, >)$ the element-wise set of inequalities for vectors a and b. Let $\mathbf{1}_n$ and $\mathbf{0}_n$ denote the vector of ones

The authors are with the Department of Mechanical and Aerospace Engineering, University of California, San Diego, CA 92093, USA, {yifuzhang,cortes}@ucsd.edu

and zeros with dimension n, respectively. For $p,q \in \mathbb{N}$, let $[p,q]_{\mathbb{N}} \triangleq \{x \in \mathbb{N} \mid p \leqslant x \leqslant q\}$. We denote the cardinality of a set σ by $|\sigma|$. Denote the unit step signal by $1(t)$. Let $I_n \in \mathbb{R}^{n\times n}$ denote the n-dimensional identity matrix. Let $\mathrm{diag}(a) \in \mathbb{R}^{n\times n}$ be the diagonal matrix whose diagonals are the elements of the vector $a \in \mathbb{R}^n$. For a matrix $A \in \mathbb{R}^{m\times n}$, $[A]_i$ denotes its ith row.

2) Algebraic graph theory: We review basic notions from algebraic graph theory from [8]. An undirected graph is a pair $\mathscr{G} = (\mathscr{I}, \mathscr{E})$, where $\mathscr{I} = \{1,\dots,n\}$ is the vertex set and $\mathscr{E} = \{e_1,\dots,e_m\} \subseteq \mathscr{I}\times\mathscr{I}$ is the edge set. A path is an ordered sequence of vertices such that any pair of consecutive vertices in the sequence is an edge of the graph. A graph is connected if there exists a path between any two vertices. Two nodes are neighbors if there exists an edge linking them. Let $\mathscr{N}(i)$ denote the set of neighbors of node i. For each edge $e_\alpha \in \mathscr{E}$ with vertices i,j, the orientation procedure consists of choosing either i or j to be the positive end of e_α and the other vertex to be the negative end. The incidence matrix $D = (d_{\alpha i}) \in \mathbb{R}^{m\times n}$ associated with $\mathscr{G}$ is defined as

$$d_{\alpha i} = \begin{cases} 1 & \text{if } i \text{ is the positive end of } e_\alpha, \\ -1 & \text{if } i \text{ is the negative end of } e_\alpha, \\ 0 & \text{otherwise.} \end{cases}$$

Define $L(Y) \triangleq D^T Y D$, where $Y \in \mathbb{R}^{m\times m}$ is an arbitrary diagonal matrix with all diagonal entries non-zero. Denote by $L^\dagger(Y)$ its unique Moore-Penrose pseudoinverse.

3) Set limit: We introduce basic definitions from set theory [9]. Suppose $\{A_k\}_{k=1}^\infty$ is a sequence of set. If

$$\bigcap_{k\geqslant 1}\bigcup_{j\geqslant k} A_j = \bigcup_{k\geqslant 1}\bigcap_{j\geqslant k} A_j = A,$$

then we say the limit of $\{A_k\}_{k=1}^\infty$ exists and is A. In shorthand notation, we write $A_k \to A$.

III. Problem Statement

This section describes the problem we are interested in solving. We start by describing the power grid mathematical model and dynamics, and then define our desired stability criteria against disturbances.

A. Power network dynamics

Following [10], [11], the power network model structure is encoded by a connected undirected graph $\mathscr{G} = (\mathscr{I}, \mathscr{E})$, where $\mathscr{I}$ corresponds to the n buses and $\mathscr{E}$ represents the m transmission lines. We denote by $P = [p_1, p_2, \dots, p_n]^T \in \mathbb{R}^n$, $\Theta = [\theta_1, \theta_2, \dots, \theta_n]^T \in \mathbb{R}^n$, and $\Omega = [\omega_1, \omega_2, \dots, \omega_n]^T \in \mathbb{R}^n$, respectively, the network power injection, the voltage angle, and the frequency vectors. In each case, the ith component of the vector corresponds to the ith node. The power network dynamics are then described by the swing equations: for each $i \in \mathscr{I}$,

$$\dot\theta_i(t) = \omega_i(t), \tag{1a}$$

$$M_i\dot\omega_i(t) = -E_i\omega_i(t) - \sum_{j\in\mathscr{N}(i)} b_{ij}\sin(\theta_i(t)-\theta_j(t)) + p_i(t), \tag{1b}$$

where $M_i > 0$ (resp. $E_i > 0$) is the moment inertia (resp. damping parameter) at node i, and b_{ij} is the susceptance of the transmission line between node i and j. For simplicity of exposition, we assume positiveness of each M_i, though our discussion can be easily extended to situations where this is not the case. Let $\Lambda(t) \triangleq D\Theta(t) \in \mathbb{R}^m$ be the voltage angle difference between every two neighboring nodes, where $D \in \mathbb{R}^{m\times n}$ is the incidence matrix corresponding to an arbitrary orientation of the graph $\mathscr{G}$. We rewrite the dynamics (1) in compact form as

$$\dot\Lambda(t) = D\Omega(t), \tag{2a}$$

$$M\dot\Omega(t) = -E\Omega(t) - D^T Y_b \mathbf{sin}(\Lambda(t)) + P(t), \tag{2b}$$

where $M \triangleq \mathrm{diag}([M_1, M_2, \dots, M_n]) \in \mathbb{R}^{n\times n}$, $E \triangleq \mathrm{diag}([E_1, E_2, \dots, E_n]) \in \mathbb{R}^{n\times n}$, $Y_b \triangleq \mathrm{diag}\{b_{ij}\} \in \mathbb{R}^{m\times m}$, and $\mathbf{sin}$ is the component-wise sine function. Under the small angle difference assumption [12], i.e., $\sin(\theta_i(t) - \theta_j(t)) \approx \theta_i(t) - \theta_j(t)$, or equivalently, $\mathbf{sin}(\Lambda(t)) \approx \Lambda(t)$, the power flow can be represented by $Y_b\Lambda(t)$ and the dynamics (2) can be linearized as follows,

$$\begin{bmatrix}\dot\Lambda(t)\\ \dot\Omega(t)\end{bmatrix} = \begin{bmatrix}\mathbf{0}_{m\times m} & D\\ -M^{-1}D^TY_b & -M^{-1}E\end{bmatrix}\begin{bmatrix}\Lambda(t)\\ \Omega(t)\end{bmatrix} + \begin{bmatrix}\mathbf{0}_m\\ M^{-1}P(t)\end{bmatrix}. \tag{3}$$

As we show later in this section, if the power injection $P(t)$ is constant, then the system (3) converges to a unique equilibrium $(\Lambda_{\mathrm{ss}}, \omega_{\mathrm{sync}}\mathbf{1}_n)$, where $\omega_{\mathrm{sync}} \in \mathbb{R}$ is called the synchronized frequency.

B. Disturbance modeling and stability criteria

We are interested in understanding how the power injection $P(t)$ influences both the transient stability and steady-state stability of the power network. For system (2) with an arbitrary initial state $(\Lambda(0), \Omega(0))$ and an arbitrary initial constant power injection $P_0 \in \mathbb{R}^n$, we consider the case where an additional power disturbance $\bar P(t,K) \in \mathbb{R}^n$ is injected into the power grid starting at time 0, i.e.,

$$P(t,K) = P_0 + \bar P(t,K), \quad \forall t \geqslant 0. \tag{4}$$

We assume the disturbance possesses the following form,

$$\bar P(t,K) = B_\rho\rho(t) + B_K D_{\zeta(t)}K, \quad \forall t \geqslant 0, \tag{5}$$

where $B_\rho \in \mathbb{R}^{n\times r}$, $B_K \in \mathbb{R}^{n\times s}$ are constant matrices; vector $\rho(t) \in \mathbb{R}^r$ (resp. $\zeta(t) \in \mathbb{R}^s$) is an integrable function with a limit denoted as $\lim_{t\to+\infty}\rho(t) = \rho_\infty$ (resp. $\lim_{t\to+\infty}\zeta(t) = \zeta_\infty$); diagonal matrix $D_{\zeta(t)}$ is a shorthand notation for the diagonal matrix $\mathrm{diag}(\zeta(t)) \in \mathbb{R}^{s\times s}$ and $K \in \mathbb{R}^s$.

The interpretation for this specific form of the disturbance are as follows. The vector $\rho(t)$ captures some known baseline disturbance, while the part $D_{\zeta(t)}K$ is some additional disturbance whose amplitude K is unknown, and whose form of trajectories are determined by $\zeta(t)$. The matrix B_ρ (resp. B_K) denotes the coupling relations between components of $\rho(t)$ (resp. $D_{\zeta(t)}K$). A simple choice could be $B_\rho = B_K = I_n$, $\rho(t) = \mathbf{0}_n$, and $\zeta(t) = 1(t)\mathbf{1}_n$, letting the disturbance $\bar P(t)$ become a step signal of amplitude K, i.e., $\bar P(t,K) = 1(t)K$. The function $\zeta(t)$ can also take the form of other types of signals, e.g., piecewise linear, exponential decaying, sinusoid signals and their (linear or nonlinear) combinations.

The problem we seek to solve is characterizing how the amplitude K in the disturbance injection affects the transient and steady-state stability of the power network. As stability criteria, we consider the following:

(i) *Transient-state frequency bound:* For a given $0 \leqslant t_1 < t_2$ and a time interval $[t_1, t_2]$, the voltage frequency $\Omega(t)$ should be upper and lower bounded by $\Omega^{\max} \in \mathbb{R}^n$ and $\Omega^{\min} \in \mathbb{R}^n$, respectively, i.e., $\Omega^{\min} \leqslant \Omega(t) \leqslant \Omega^{\max}, \quad \forall t \in [t_1, t_2]$.

(ii) *Transient-state power flow bound:* For any given time interval $[t_1, t_2]$, the power flow $Y_b\Lambda(t)$ should be upper and lower bounded by $F^{\max} \in \mathbb{R}^m$ and $F^{\min} \in \mathbb{R}^m$, respectively, i.e., $F^{\min} \leqslant Y_b\Lambda(t) \leqslant F^{\max}, \quad \forall t \in [t_1, t_2]$.

(iii) *Steady-state synchronized frequency bound:* At steady state, the synchronized frequency ω_{sync} should be upper and lower bounded by $\omega_{\text{sync}}^{\max} \in \mathbb{R}$ and $\omega_{\text{sync}}^{\min} \in \mathbb{R}$, respectively, i.e., $\omega_{\text{sync}}^{\min} \leqslant \omega_{\text{sync}} \leqslant \omega_{\text{sync}}^{\max}$.

(iv) *Steady-state power flow bound:* At steady state, the power flow $Y_b\Lambda_{\text{ss}}$ should be upper and lower bounded by $F_{\text{ss}}^{\max} \in \mathbb{R}^m$ and $F_{\text{ss}}^{\min} \in \mathbb{R}^m$, respectively, i.e., $F_{\text{ss}}^{\min} \leqslant Y_b\Lambda_{\text{ss}} \leqslant F_{\text{ss}}^{\max}$.

We refer to the set Ψ^T of all $K \in \mathbb{R}^s$ satisfying requirements (i)-(ii) as the transient-state feasibility set. Similarly, we refer to the set Ψ^S of all $K \in \mathbb{R}^s$ satisfying requirements (iii)-(iv) as the steady-state feasibility set. A vector K that lies in $\Psi^T \cap \Psi^S$ does not destroy either the transient-state constraints or the steady-state constraints for the power network. Our objective is then to provide formal descriptions of these sets.

Remark 3.1: (Computation of the steady-state feasibility set). We show that the steady-state feasibility set Ψ^S can be equivalently expressed in the following form. First define

$$P_\infty \triangleq P_0 + B_\rho \rho_\infty + B_K D_{\zeta_\infty} K, \ \omega_{\text{sync}} \triangleq \mathbf{1}_n^T P_\infty / \sum_{i=1}^n E_i, \quad \text{(6a)}$$

$$L(Y_b) \triangleq D^T Y_b D, \ \Lambda_{\text{ss}} \triangleq D L^\dagger(Y_b)\left(P_\infty - \omega_{\text{sync}} E \mathbf{1}_n\right). \quad \text{(6b)}$$

One can show [13] that the system (3) with input (5) convergences to the unique equilibrium $(\Lambda_{\text{ss}}, \omega_{\text{sync}}\mathbf{1}_n)$. Hence $K \in \Psi^S$ if and only if

$$\omega_{\text{sync}}^{\min} \leqslant \omega_{\text{sync}} \leqslant \omega_{\text{sync}}^{\max},$$
$$F_{\text{ss}}^{\min} \leqslant Y_b D L^\dagger(Y_b)\left(P_\infty - \omega_{\text{sync}} E \mathbf{1}_n\right) \leqslant F_{\text{ss}}^{\max},$$

where P_∞ and ω_{sync} are both linear functions of K, as defined in (6). It is easy to see that the set Ψ^S is a s-dimensional convex polytope consisting of $m+1$ constraints. •

IV. Computation of the transient-state feasibility set

In this section we start by illustrating how the computation of the transient-state feasibility set is a hard problem in general. Our strategy to deal with this is to turn them into obtaining inner and outer approximations of this set that are easier to compute, and whose degree of exactness can be tuned by the designer.

We start by re-writing the dynamics (3) with input (4) as follows,

$$\dot{x}(t,K) = Ax(t,K) + \begin{bmatrix} \mathbf{0}_m \\ M^{-1}P(t,K) \end{bmatrix}, \quad \text{(8a)}$$

where

$$x(t,K) = \begin{bmatrix} \Lambda(t,K) \\ \Omega(t,K) \end{bmatrix}, \ A = \begin{bmatrix} \mathbf{0}_{m\times m} & D \\ -M^{-1}D^T & -M^{-1}E \end{bmatrix}.$$

Solving (8), one has

$$x(t,K) = e^{At}x_0 + \int_0^t e^{A(t-\tau)} \begin{bmatrix} \mathbf{0}_m \\ M^{-1}P(\tau,K) \end{bmatrix} \mathrm{d}\tau = S(t) + V(t)K,$$

where

$$S(t) \triangleq e^{At}x_0 + \int_0^t e^{A(t-\tau)} \begin{bmatrix} \mathbf{0}_m \\ M^{-1}\left(P_0 + B_\rho \rho(\tau)\right) \end{bmatrix} \mathrm{d}\tau,$$
$$V(t) \triangleq \int_0^t e^{A(t-\tau)} \begin{bmatrix} \mathbf{0}_m \\ M^{-1}B_K D_{\zeta(\tau)} \end{bmatrix} \mathrm{d}\tau.$$

Denoting

$$x^{\max} \triangleq \begin{bmatrix} \Omega^{\max} \\ F^{\max} \end{bmatrix}, \ x^{\min} \triangleq \begin{bmatrix} \Omega^{\min} \\ F^{\min} \end{bmatrix},$$

one can express the transient-state feasibility set as

$$\Psi^T = \left\{ K \in \mathbb{R}^s \,\middle|\, x^{\min} \leqslant S(t) + V(t)K \leqslant x^{\max}, \quad \forall t \in [t_1, t_2] \right\}.$$

This expression shows that Ψ^T consists of infinitely many affine constraints of K and hence is convex. Due to the infinitely many constraints in Ψ^T, here we provide instead inner and outer approximations of Ψ^T that are easy to compute. The inner approximation is based on the idea of requiring the constraints in Ψ^T be satisfied at a finite collection of time points but with narrowed bound limits, and thus making sure that the ones unchecked are not violated. The outer approximation is simply a subset of the constraints appearing in Ψ^T.

A. Transient-state feasibility set for a scalar signal

Here, we restrict our attention to scalar signals. We later build on this analysis to address the more general case of vector signals.

Consider a time-dependent differentiable real signal $t \mapsto y(t,K)$ and a sequence of time

$$\tau = \left\{ (\tau_1, \tau_2, \ldots, \tau_r) \,\middle|\, t_1 = \tau_1 < \tau_2 < \ldots < \tau_r = t_2 \right\}. \quad \text{(10)}$$

We want to know what kinds of K guarantee that

$$y^{\min} \leqslant y(t,K) \leqslant y^{\max}, \quad \forall t \in [t_1, t_2]. \quad \text{(11)}$$

Suppose that there exists a real signal $t \mapsto y_d(t,K) \in \mathbb{R}$ such that it can upper-bound the derivative of $y(t,K)$, i.e.,

$$|\dot{y}(t,K)| \leqslant y_d(t,K), \quad \forall t \in [t_1, t_2]. \quad \text{(12)}$$

The next result shows that if $y_d(t,K)$ is bounded, then one can ensure (11) by only restricting the value of $y(t,K)$ for $t \in \tau$.

Lemma 4.1: (Sufficient condition for checking real-time state constraint). For a sequence of time τ defined in (10), a time-dependent differentiable real signal $t \mapsto y(t,K)$, and a derivative bound signal $t \mapsto y_d(t,K)$ defined in (12), assume that $y_d(t,K)$ can be bounded independent with t and for each $q \in [1, r-1]_{\mathbb{N}}$, define $d_q(K) \triangleq \max_{t\in[\tau_q,\tau_{q+1}]}\{y_d(t,K)\} \in \mathbb{R}$. Let $\delta_q(K) \triangleq d_q(K)(\tau_{q+1} - \tau_q)/2 \in \mathbb{R}$. If

$$y^{\min} + \delta_q(K) \leqslant y(\tau_q, K) \quad \leqslant y^{\max} - \delta_q(K), \quad \text{(13a)}$$

$$y^{\min} + \delta_q(K) \leqslant y(\tau_{q+1}, K) \leqslant y^{\max} - \delta_q(K), \tag{13b}$$

for all $q \in [1, r-1]_{\mathbb{N}}$, then (11) holds.

Given the time signal y, Lemma 4.1 opens the way to efficiently compute inner and outer approximations for the set

$$\Sigma \triangleq \left\{ K \,\middle|\, y^{\min} \leqslant y(t,K) \leqslant y^{\max}, \quad \forall t \in [t_1, t_2] \right\}. \tag{14}$$

The next result formally states this, and shows that the two approximations can be arbitrarily accurate by adapting ε^τ defined as the largest time period in τ. i.e.,

$$\varepsilon^\tau \triangleq \max_{q \in [1,r-1]_{\mathbb{N}}} \{\tau_{q+1} - \tau_q\} > 0. \tag{15}$$

Lemma 4.2: (Inclusion relations and convergence of inner and outer set). Under the assumption in Lemma 4.1, further assume that there exists a bounded $\tilde{d}_q$ independent with K such that $d_q(K) \leqslant \tilde{d}_q$ for all $q \in [1, r-1]_{\mathbb{N}}$. Denote

$$\begin{aligned}
&\tilde{\delta}_q \triangleq \tilde{d}_q(\tau_{q+1} - \tau_q)/2, \\
&\Sigma_O \triangleq \left\{ K \,\middle|\, y^{\min} \leqslant y(\tau_q, K) \leqslant y^{\max}, \quad \forall q \in [1, r]_{\mathbb{N}} \right\}, \\
&\Sigma_I \triangleq \Big\{ K \,\Big|\, y^{\min} + \tilde{\delta}_q \leqslant y(\tau_q, K),\ y(\tau_{q+1}, K) \\
&\qquad\qquad \leqslant y^{\max} - \tilde{\delta}_q, \quad \forall q \in [1, r-1]_{\mathbb{N}} \Big\}.
\end{aligned}$$

It holds that

(i) $\Sigma_I \subseteq \Sigma \subseteq \Sigma_O$, and
(ii) if $\varepsilon^\tau \to 0^+$, then $\Sigma_O \to \Sigma$ and $\Sigma_I \to \Sigma$.

B. Metric measuring the approximation gap

An interesting question regarding using Σ_I and Σ_O to approximate Σ is how well the approximation is. If we define

$$\begin{aligned}
\bar{\Sigma}_O \triangleq \Big\{ K \,\Big|\, & y^{\min} - 2\tilde{\delta}_q \leqslant y(t,K) \leqslant \\
& y^{\max} + 2\tilde{\delta}_q,\ \forall t \in [\tau_q, \tau_{q+1}],\ \forall q \in [1, r-1]_{\mathbb{N}} \Big\}, \quad (17a) \\
\bar{\Sigma}_I \triangleq \Big\{ K \,\Big|\, & y^{\min} + \tilde{\delta}_q \leqslant y(t,K) \leqslant \\
& y^{\max} - \tilde{\delta}_q,\ \forall t \in [\tau_q, \tau_{q+1}],\ \forall q \in [1, r-1]_{\mathbb{N}} \Big\}, \quad (17b)
\end{aligned}$$

then one has that for a same τ, It holds that $\bar{\Sigma}_I \subseteq \Sigma_I \subseteq \Sigma \subseteq \Sigma_O \subseteq \bar{\Sigma}_O$. Therefore a conservative but guaranteed way to describe the approximation extent is to depict the gap between $\bar{\Sigma}_I$ and Σ, and between Σ and $\bar{\Sigma}_O$. Since $\bar{\Sigma}_I$ and $\bar{\Sigma}_O$ almost have the same structure with difference coming only from shifted upper and lower bound, we here, for simplicity, only show a metric describing the gap between $\bar{\Sigma}_I$ and Σ. We define our approximation extent metric as,

$$\nu(\tau) \triangleq \max_{q \in [1,r-1]_{\mathbb{N}}} \{\tilde{\delta}_q\}. \tag{18}$$

An explanation of choosing ν as the metric is as follows. For a given $q \in [1, r-1]_{\mathbb{N}}$, define $cns(\tilde{\delta}_q)$ as the collection of all $K's$ that satisfy $y^{\min} \leqslant y(t,K) \leqslant y^{\max},\ \forall t \in [\tau_q, \tau_{q+1}]$ while not satisfy $y^{\min} + \tilde{\delta}_q \leqslant y(t,K) \leqslant y^{\max} - \tilde{\delta}_q,\ \forall t \in [\tau_q, \tau_{q+1}]$. It holds that,

$$cns(\tilde{\delta}_q) \subseteq \left\{ K \,\middle|\, y^{\min} \leqslant y(t,K) \leqslant y^{\min} + \tilde{\delta}_q, \right.$$
$$\left. y^{\max} - \tilde{\delta}_q \leqslant y(t,K) \leqslant y^{\max}, \quad \forall t \in [\tau_q, \tau_{q+1}] \right\}. \tag{19}$$

It is easy to see that the region $cns(\tilde{\delta}_q)$ becomes smaller as $\tilde{\delta}_q$ decreases, and becomes empty as $\tilde{\delta}_q$ is 0. Hence a good metric to measure the size of $cns(\tilde{\delta}_q)$ would simply be $\tilde{\delta}_q$. Also since $\Sigma \backslash \bar{\Sigma}_I \subseteq \bigcup_{q \in [1,r-1]_{\mathbb{N}}} cns(\tilde{\delta}_q)$, the meaning of $\nu(\tau)$ is clear: it stands for the largest conservativeness region among all $[\tau_q, \tau_{q+1}]$ intervals. Lastly, it should be mentioned that i) the proposed metric $\nu(\tau)$ works symmetrically for measuring the gap between $\bar{\Sigma}_O$ and Σ as well, and ii) if $\nu(\tau) \to 0^+$, then $\bar{\Sigma}_I \to \Sigma$ and hence $\Sigma_I \to \Sigma$.

C. Algorithm to reduce the approximation gap

One obvious way to reduce $\nu(\tau)$ and hence make both Σ_O and Σ_I more similar to Σ is to add more sampling points into τ, but this way would inevitably increase the number of constraints appeared in both Σ_I and Σ_O, making the two sets more complicated; therefore, an interesting issue would be how to find a relative small $\nu(\tau)$ if the number of sampling points (i.e., r) is fixed. Since in general ν is a non-convex function, finding the minimal value and its optimal solution set can be intractable or NP-hard; however, it is still possible to reasonably adjust the sampling sequence τ to attain a smaller metric value. The following algorithm, starting from an arbitrary initial sampling sequence $\tau^0 = \{\tau_1^0, \tau_2^0, \ldots, \tau_r^0\}$ as defined in (10), is able to monotonically decrease the metric value by modifying the sampling points until termination. Furthermore, denote $\tilde{d}_{\max} \triangleq \max_{q \in [1,r-1]_{\mathbb{N}}} \tilde{d}_q$ and let $\bar{\tau}$ be the sampling sequence generated as Algorithm 1 terminate, then if $\tilde{d}_{\max}$ is independent with the sampling sequence, we can upper bound $\nu(\bar{\tau})$ with respect to $\tilde{d}_{\max}$.

Algorithm 1: Reduce metric value

Data: A sampling sequence $\tau^0 = \{\tau_1^0, \tau_2^0, \ldots, \tau_r^0\}$, where $t_1 = \tau_1^0 < \tau_2^0 < \ldots < \tau_r^0 = t_2$; derivative bound signal y_d defined in (12)
Result: An improved sampling sequence $\bar{\tau} \triangleq \{\bar{\tau}_1, \bar{\tau}_2, \ldots, \bar{\tau}_r\}$ such that $\bar{\tau}_1 = t_1,\ \bar{\tau}_r = t_2$, and $\nu(\bar{\tau}) \leqslant \nu(\tau^0)$;

```
Initialization: τ ≜ {τ_1, τ_2, ..., τ_r} = τ^0
while not terminated do
    for q = 1 : r − 2 do
        d̃_{q,q+1} ≜ max{d̃_q, d̃_{q+1}}
        μ_q ≜ d̃_{q,q+1}(τ_{q+2} − τ_q)/2
    end
    Compute μ_max ≜ min_{q∈[1,r−2]_N}{μ_q}; select any q' that belongs to its optimal solution set; select any q* that solves max_{q∈[1,r−1]_N}{δ̃_q}
    if μ_max < ν(τ) then
        Update the sampling sequence τ by deleting the sampling point τ_{q'+1} and then by adding a sampling point in the middle of [τ_{q*}, τ_{q*+1}]
    else
        τ̄ = τ; quit the algorithm
    end
end
```

Next we show the monotonic decreasing property of the value of ν obtained in each round of Algorithm 1 and provide an upper bound of $\nu(\bar{\tau})$ for arbitrary initial time sequence τ^0.

Lemma 4.3: (Properties of Algorithm 1). Suppose $r \geqslant 3$, then for an arbitrary initial sampling time sequence τ^0 defined in (10), it holds that

(i) If at some round of the algorithm, the sampling sequence is updated from τ to τ', then $\nu(\tau') \leqslant \nu(\tau)$.
(ii) $\nu(\bar{\tau}) \leqslant \tilde{d}_{\max}(t_2 - t_1)/(r-2)$.

D. Approximation of the transient-state feasibility set

Based on Lemma 4.2, we are finally ready to depict the set Ψ^T by two sets that sandwich Ψ^T.

Theorem 4.4: (Inclusion relations and convergence of inner and outer set for the transient-state stability set). Suppose the vector K can be bounded such that $\|K\|_\infty \leqslant \gamma$. Further let

$$
\begin{aligned}
R(t) &\triangleq Ae^{At}\left(x_0 + \int_0^t e^{-A\tau}\begin{bmatrix}\mathbf{0}_m \\ M^{-1}\left(P_0 + B_\rho \rho(\tau)\right)\end{bmatrix} \mathrm{d}\tau\right) \\
&\quad + \begin{bmatrix}\mathbf{0}_m \\ M^{-1}\left(P_0 + B_\rho \rho(t)\right)\end{bmatrix}, \\
Q(t) &\triangleq Ae^{At}\int_0^t e^{-A\tau}\begin{bmatrix}\mathbf{0}_m \\ M^{-1}B_K D_\zeta(\tau)\end{bmatrix}\mathrm{d}\tau + \begin{bmatrix}\mathbf{0}_m \\ M^{-1}B_K D_\zeta(t)\end{bmatrix}, \\
z_i(t) &\triangleq |[R(t)]_i| + \gamma \|[Q(t)]_i\|_1, \quad \forall i \in [1, n+m]_{\mathbb{N}}. \qquad (20)
\end{aligned}
$$

For every $i \in [1, n+m]_{\mathbb{N}}$, choose any sampling sequence $\tau^i = \{\tau_1^i, \tau_2^i, \ldots, \tau_{r(i)}^i\}$ defined in (10), and define

$$
\begin{aligned}
&\varepsilon^{\tau^i} \triangleq \max_{q \in [1, r(i)-1]_{\mathbb{N}}} \{\tau_{q+1}^i - \tau_q^i\} > 0, \\
&\tilde{d}_{q,i} \triangleq \max_{t \in [\tau_q^i, \tau_{q+1}^i]} \{z_i(t)\}, \quad \forall q = [1, r(i)-1]_{\mathbb{N}}, \\
&\tilde{\delta}_{q,i} \triangleq \tilde{d}_{q,i}(\tau_{q+1}^i - \tau_q^i)/2, \quad \forall q = [1, r(i)-1]_{\mathbb{N}}, \\
&\Psi_{O,i}^T \triangleq \Big\{ K \;\Big|\; x_i^{\min} \leqslant [S(\tau_q^i)]_i + [V(\tau_q^i)]_i K \\
&\qquad\qquad \leqslant x_i^{\max}, \quad \forall q \in [1, r(i)]_{\mathbb{N}} \Big\}. \\
&\Psi_{I,i}^T \triangleq \Big\{ K \;\Big|\; x_i^{\min} + \tilde{\delta}_{q,i} \leqslant [S(\tau_q^i)]_i + [V(\tau_q^i)]_i K, \; [S(\tau_{q+1}^i)]_i \\
&\qquad + [V(\tau_{q+1}^i)]_i K \leqslant x_i^{\max} - \tilde{\delta}_{q,i}, \quad \forall q \in [1, r(i)-1]_{\mathbb{N}} \Big\},
\end{aligned}
$$

$$
\Psi_O^T \triangleq \bigcap_{i \in [1, n+m]_{\mathbb{N}}} \Psi_{O,i}^T, \quad \Psi_I^T \triangleq \bigcap_{i \in [1, n+m]_{\mathbb{N}}} \Psi_{I,i}^T.
$$

It holds that

(i) $\Psi_I^T \subseteq \Psi^T \subseteq \Psi_O^T$, and
(ii) If $\varepsilon^{\tau^i} \to 0^+$ for all $i \in [1, m+n]_{\mathbb{N}}$, then $\Psi_O^T \to \Psi^T$ and $\Psi_I^T \to \Psi^T$.

Similar to the way we define ν in (18), here we define

$$
\begin{aligned}
&\pi_i \triangleq \max_{q \in [1, r(i)]_{\mathbb{N}}} \{\tilde{\delta}_{q,i}\}, \\
&\pi \triangleq \max_{i \in [1, m+n]_{\mathbb{N}}} \{\pi_i / (x_i^{\max} - x_i^{\min})\}, \qquad (22)
\end{aligned}
$$

and use π as the metric measuring the approximation gap, where the coefficient $1/(x_i^{\max} - x_i^{\min})$ scales π_i relative to its bounds. Still we can reduce π by reducing every π_i independently using Algorithm 1.

parameter	value	parameter	value
M	I_{118}	t_0	$0s$
Y_b	$8I_{186}$	t_1	$4s$
E	$0.2I_{118}$	γ	0.65
$F^{\max}$ and $-F^{\min}$	$2.4\mathbf{1}_{186}$	$\Omega^{\max}$ and $-\Omega^{\min}$	$0.1\mathbf{1}_{118}$

TABLE I: Power network parameters.

V. Simulations

In this section, we illustrate our results on the IEEE 118-bus power network [14], which has 54 generators, 91 loads and 186 transmission lines. We run our simulations in MATLAB on a laptop with a 3GHz Intel Core i7 dual-core CPU and 8GB of RAM. We select parameters based on [11], [15] with minor adjustments, cf. Table I. The initial power injection vector P_0 is as follows: the initial power injection of all 54 generators is 1, of all 91 loads is -54/91, and of all other nodes is 0. We also set $\Omega(0) = \mathbf{0}_{118}$ and $\Lambda(0) = DL^\dagger(Y_b)P_0$. The order and directions of the transmission lines can be arbitrary, since all lines have the same transient-state maximum bound and minimum bound, where the two bounds have the same absolute value. Under this setup, at $t = 0$, the system (3) is balanced. At that time instant, a disturbance in the form of step signals with amplitude K_1 (resp. K_2) is injected into node 34 (resp. node 35), i.e., $[\bar{P}(t,K)]_i = 1(t)K_1$ (resp. $[\bar{P}(t,K)]_i = 1(t)K_2$) if $i = 34$ (resp. $i = 35$), and all other components of $\bar{P}(t,K)$ are zero.

In Figure 1 (a) to (d), the gray regions with dotted boundaries represent Ψ_I^T, while the yellow regions with solid boundaries stand for Ψ_O^T. As Theorem 4.4 states, the transient-state feasibility set Ψ^T is contained in Ψ_O^T and contains Ψ_I^T. In (a), the sampling sequence τ^i for each state x_i is chosen to be the same one with even sampling period 0.2s, i.e., $\tau^i = \{0s, 0.2s, 0.4s, \ldots, 3.8s, 4s\}$, $\forall i \in [1, m+n]_{\mathbb{N}}$, while in (b), each sampling sequence is optimized by Algorithm 1, and we use $\{0s, 0.2s, 0.4s, \ldots, 3.8s, 4s\}$ as the initial sampling sequence for all $i \in [1, m+n]_{\mathbb{N}}$. By optimizing the sampling sequences (but maintaining the same number of sampling points), the gap between Ψ_I^T and Ψ_O^T is smaller in (b) than in (a). In (b) to (d), we still apply Algorithm 1 to optimize the sampling sequence, but increase the number of sampling points. In particular, we still choose even sampling sequence to initiate Algorithm 1 but decrease its sampling period from $0.2s$ as in (b), $0.1s$ as in (c), to $0.05s$ as in (d). We observe convergence between the two approximations, which verifies statement (ii) in Theorem 4.4.

Lastly, we illustrate how the total computation time for the approximations Ψ_O^T and Ψ_I^T (resp. the metric value π) changes with the number of sampling points and the size of the disturbance. In each data point of Figure 2(a)-(b), we use the same even sampling sequence for each $i \in [1, m+n]_{\mathbb{N}}$ and optimize the sequence using Algorithm 1. For different data points, we decrease the sampling period from 0.2s to 0.05s, in 0.025 decrements. As a comparison, in Figure 2(c)-(d), we repeat the simulations for disturbances injected at all 91 load nodes in the form of step signal with amplitude K, i.e., for the

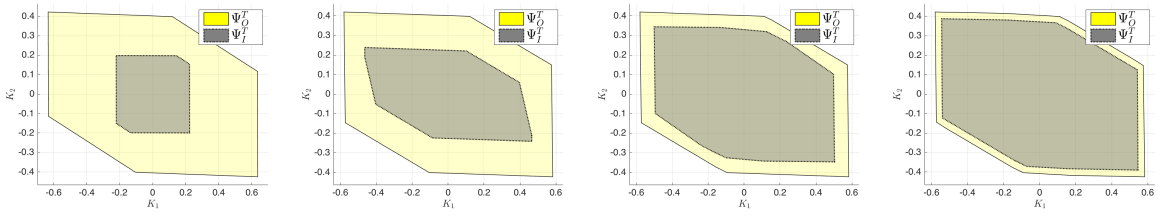

(a) (b) (c) (d)

Fig. 1: Inner and outer approximations of the transient-state feasibility set with different sampling sequences.

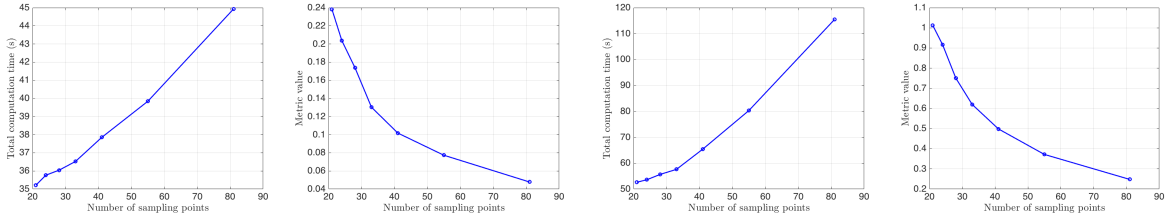

(a) (b) (c) (d)

Fig. 2: Illustration of the total time to compute the inner and outer approximations and the metric value with respect to different numbers of sampling points.

jth load node, $[\bar{P}(t,K)]_j = 1(t)K_j$, and all other components of $\bar{P}(t,K)$ are zero. Comparing (a) and (c), though the number of disturbances with amplitude K increases sharply from 2 to 91, the total computation time remains acceptable. However, for the same number of sampling points, the metric value associated with the 91-disturbance case is higher than that with the 2-disturbance case. This is because the increase in the number of disturbances makes $z_i(t)$ in (20), the estimation of the derivative bound of $x_i(t)$, become larger for some $i \in [1, m+n]_{\mathbb{N}}$, resulting in an increase of π_i in (22), and finally boosting the metric π.

VI. Conclusions

We have considered the problem of efficiently describing the set of disturbances to a power network that do not affect its transient-state and steady-state stability in terms of frequency and power flow. Under the assumption that a bound on the amplitude of the disturbance is available, we have devised a sampling method to provide superset and subset approximations of the transient-state feasibility set. These approximations can be computed with arbitrary accuracy, at the cost of increasing the computational complexity. We have also introduced a metric to measure the approximation gap and designed an algorithm to optimize it for a given fixed number of sampling points. Future work will investigate the definition of robustness margins for the power network based on the feasibility sets, provide approximations for systems with uncertain baseline disturbances, extend the analysis from constant amplitude to time-varying amplitude, and quantify the difference between the feasibility sets of the nonlinear swing dynamics and its linearized version.

Acknowledgments

This work was partially supported by NSF award CNS-1329619 and AFOSR Award FA9550-10-1-0499.

References

[1] P. Kundur, J. Paserba, V. Ajjarapu, G. Andersson, A. Bose, C. Canizares, N. Hatziargyriou, D. Hill, A. Stankovic, C. Taylor, T. V. Cutsem, and V. Vittal, "Definition and classification of power system stability," *IEEE Transactions on Power Systems*, vol. 19, no. 2, pp. 1387–1401, 2004.

[2] A. Gajduk, M. Todorovski, and L. Kocarev, "Stability of power grids: an overview," *The European Physical Journal Special Topics*, no. 223, pp. 2387–2409, 2014.

[3] M. Pavella, D. Ernst, and D. Ruiz-Vega, *Transient Stability of Power Systems: A Unified Approach to Assessment and Control*. Kluwer Academic Publishers, 2012.

[4] A. Pai, *Energy Function Analysis for Power System Stability*. Springer, 1989.

[5] H. D. Chiang, *Direct Methods for Stability Analysis of Electric Power Systems: Theoretical Foundation, BCU Methodologies, and Applications*. John Wiley and Sons, 2011.

[6] Y. Zhang and J. Cortés, "Quantifying the robustness of power networks against initial failure," in *European Control Conference*, Aalborg, Denmark, July 2016, pp. 2072–2077.

[7] Q. Ba and K. Savla, "On decentralized robust weight control for DC power networks," in *American Control Conference*, Boston, MA, July 2016, pp. 5933–5938.

[8] F. Bullo, J. Cortés, and S. Martínez, *Distributed Control of Robotic Networks*, ser. Applied Mathematics Series. Princeton University Press, 2009, electronically available at http://coordinationbook.info.

[9] S. I. Resnick, *A Probability Path*. Birkhäuser Boston, 1998.

[10] C. Zhao, E. Mallada, and F. Dorfler, "Distributed frequency control for stability and economic dispatch in power networks," in *American Control Conference*, Chicago, IL, 2015, pp. 2359–2364.

[11] N. Li, L. Chen, C. Zhao, and S. H. Low, "Connecting automatic generation control and economic dispatch from an optimization view," in *American Control Conference*, Portland, OR, June 2014, pp. 735–740.

[12] A. R. Bergen and V. Vittal, *Power System Analysis*. Upper Saddle River, NJ: Prentice Hall, 2000.

[13] E. Mallada, "Distributed network synchronization: The internet and electric power grids," Ph.D. dissertation, Cornell University, 2014, electronically available at http://www.its.caltech.edu/ mallada/pubs/2014/thesis.pdf.

[14] http://motor.ece.iit.edu/data/JEAS_IEEE118.doc.

[15] P. J. Menck, J. Heitzig, J. Kurths, and H. J. Schellnhuber, "How dead ends undermine power grid stability," *Nature Communications*, vol. 5, no. 3969, pp. 1–8, 2014.